Depollution of Synthetic dyes From Waste Water Using Polyazomethine/TiO_2 And Polyazomethine/ZnO Nanocomposites Via Photocatalytic Process

Pradeeba S J [1*], Sampath [2]

[1]Department of Chemistry, Hindusthan College of Engineering and Technology, Coimbatore, Tamil Nadu, India.

[2]Department of Chemistry, Kumaraguru College of Technology, Coimbatore, Tamil Nadu, India

[*]Corresponding author: Pradeeba S J

E-mail: pradeebasj@gmail.com, tel: 9942560573

GRAPHICAL ABSTRACT

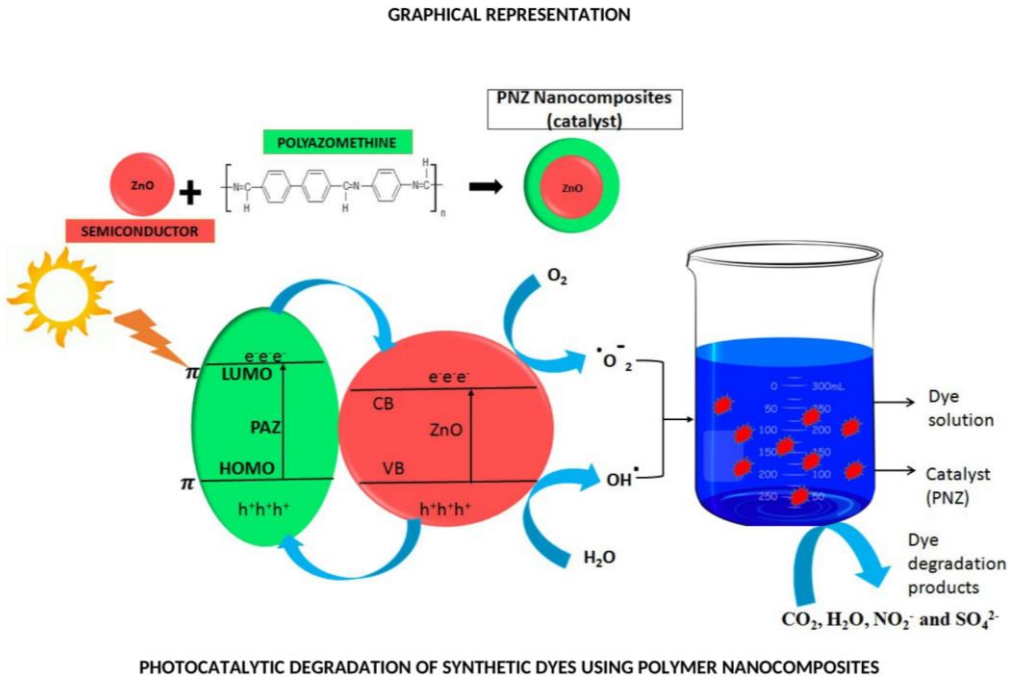

ABSTRACT

We propose a simple method for synthesising Poly(azomethine), ZnO, TiO_2, poly(azomethine)/TiO_2, and poly(azomethine)/ZnO nanocomposites using an ultrasonication process, as well as the use of these nanomaterials for photocatalytic degradation of organic dyes

(Methylene blue (MB), malachite green (MG), Bismarck brown (BB), alizarin red S (ARS), and (MO). Our findings show that precise control and optimization of ambient factors in the presence of natural sunlight can result in efficient tailoring of poly(azomethine)/TiO_2 (PNT) and poly(azomethine)/ZnO (PNZ) nanocomposites. Compared to Poly(azomethine), ZnO, TiO catalysts, the PNT and PNZ composites exhibit better photocatalytic activity for MB, MG, BB, ARS, MO degradation, which could be attributed to the formation of special catalytically active structures on the nanocomposite surface. The synthesized PNT and PNZ composites had the maximum catalytic activity under circumstances of 500 mg photocatalyst dose, 5 h of sunlight exposure and 10 ppm dye concentrations. Under ideal conditions, MB degrades at a rate of 97 % after 5 h of sunlight exposure. The composites demonstrated selective dye degradation and have greater photocatalytic effectiveness for cationic dyes. This research could lead to the simple development of a high photocatalysts for the rapid removal of ecologically harmful dyes from aqueous solutions.

Keywords: Organic dyes, sunlight irradiation, degradation efficiency, cationic dyes, anionic dyes, stability and reusability.

1. Introduction

Synthetic organic dyes are used in a variety of industries, including textiles, leather finishing, food, paper production, pharmaceuticals, medicine, photography, cosmetics, hair colouring, agricultural, biological, chemical research and light harvesting arrays. Our main source of wastewater effluent is harmful compounds, which contain roughly 72 distinct substances, with nearly 32 of them being untreatable. According to a recent survey conducted by the Ecological and Toxicological Association of Dyestuffs and Manufacturing Industry (ETAD), 90% of dyes screened from various sources (diazo, direct, and basic) were found to be lethal with a value greater than 2 x 10^3 mg/kg and a high toxic nature (Lakshmiprasanna and Rajagopalan, 2016; Mzoughi *et al*., 2016). Highly intense coloured water dissolvable dyestuffs are spontaneous and acid dyes are complicated to eradicate from the water. The low concentration and period of exposure affects transparency and

gas solubility resulting in considerable reduction in photosynthesis process and decreases soil quality and affects plant growth (Perju *et al*., 2015; Ahmad *et al*., 2022). In India, a major source of metal contamination in topsoil is from textile dye industrial waste (Riaz *et al*., 2015). The colour in water bodies hides other different types of pollution. Chemical oxygen demand (COD), total dissolved solids (TDS), pH inconsistency, and biological reagent degradability are all characteristics of dye wastewater. Human intake of such contaminated water results in wide range of health hazards such as breathing problems, immune suppression, central nervous system disorder, allergic reactions, tissue necrosis and infections in eyes and skin (Al-Kahtani, 2017; Amenaghawon *et al*.,2014). Hence it is mandatory to remove dyes from wastewater in such a way that both colour and toxicity should get eliminated completely.

To improve the photodegradation property of the semiconductor material, composite materials are equipped by using a semiconductor material. A dopant is generally incorporated into the crystal lattice plane of the semiconductor nanomaterial which can enhance the effective photodegradation, effortless departure of catalysts, elevated exterior area and efficient electron-hole recombination (Patil and Shrivastava, 2015; Liuxue *et al*., 2006), . Mainly materials such as zeolite, activated carbon, carbon nanotubes, graphene, conducting polymers were used to prepare a composite material with an effective nanostructured semiconductor material. Since these materials results in the effective charge transfer properties which helps in the efficacy of the dye degradation. Such composite materials are discussed below in detail with their change in physiochemical properties and enhancement in dye degradation. Most toxic synthetic organic dyes were tested as a sample dye to find out the stability and capability of the newly synthesized composite material (Zhu *et al*., 2010; Pathania *et al*., 2016).

The primary goal of this study is to create a polymeric nanocomposite material made up of a chelating polymer with azomethine linkages and an inorganic semiconductor material that can act as a dopant (Huili and Chang, 1991; Ansari *et al*., 2015). After that, the photocatalytic applications with various acidic and basic dyes were carried out using the produced polymeric nanocomposites.

Because of their increased dye degradation ability and higher stability, these synthetic polymeric nanocomposites could be a suitable option in the future.

2. Materials and methods

All of the chemicals used in the synthesis were purchased and used directly from Sigma Aldrich.

2.1. Synthesis of 4, 4'-diformyl biphenyl monomer

The monomer synthesis is shown in Scheme-1. Hexamethylenetetramine (6.8 g) was dissolved in 90 mL ethanol in a round bottom flask. At 40°C, 3, 4'-bis (chloromethyl) biphenyl (3.0 g) was gently added to the ethanolic mixture. The slurry mixture was agitated for 90 minutes using a magnetic stirrer, and the temperature was gradually raised to 50 °C. The precipitate was collected and rinsed with ethanol numerous times. A total of 40 mL of 50% acetic acid was added and refluxed for 10 h. The filtrate was chilled overnight in a desiccator after the mixture was filtered.

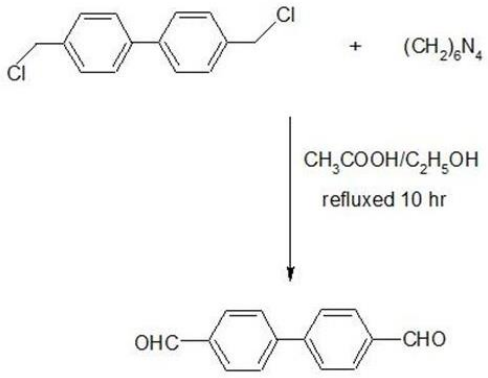

Scheme-1 Synthesis of monomer 4, 4'-Bis (formyl) biphenyl

2.2. Synthesis of Polyazomethine (PAZ)

The polymer synthesis is based on the reference work carried out by Vasanthi and Ravikumar, 2013. About 0.5 mol of 4, 4'-diformyl biphenyl monomer is taken in DMF medium added slowly into a mixture of toluene solution of 0.5 mol p-phenylenediamine. The contents of the reaction were refluxed for 6 h and then allowed to cool before being discharged into methanol. The resultant precipitate was filtered and dried (Scheme-2).

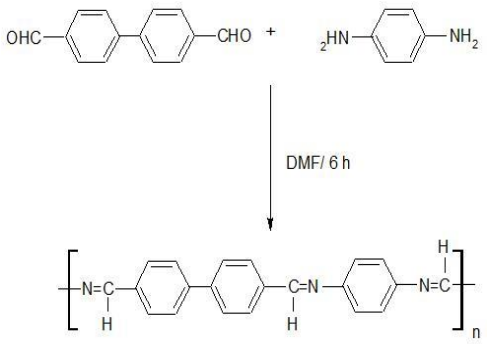

Scheme-2 Synthesis of polyazomethine (PAZ)

2.3. Synthesis of ZnO nanoparticle

Under vigorous stirring, an aqueous solution of KOH (0.4 M) is gradually discharged into a zinc nitrate solution (0.2 M) at room temperature, resulting in the formation of a white suspension. After being rinsed three times with filtered water, the whitish substance was centrifuged. Finally, the produced product was rinsed in pure alcohol before being calcined for 3 hours at 500 degrees Celsius.

2.4.Synthesis of TiO_2 nanoparticle

In an ice bath, $TiCl_4$ was gradually added to clean water with stirring until it was entirely dissolved simultaneously add NH_4OH (30%) solution was added. After 1 hour, the white TiO_2 nanoparticle was filtered. Obtained TiO_2 nanoparticles were washed in clean water and dehydrated for 3 h under vacuum at 100°C.

2.5.Synthesis of ZnO/TiO_2 incorporated polyazomethine polymeric nanocomposite

500 mg polyazomethine is dissolved in 100 mL DMF solution and sonicated for 48 hours under constant stirring. Under sonication, ZnO or TiO_2 nanoparticles are liberated in acetone and simultaneously added to the polymeric solution. The precipitated ZnO incorporated polyazomethine (PNZ) or TiO_2 incorporated polyazomethine (PNT) composite material is filtered, washed repeatedly in acetone and dried out (PNT & PNZ) (Fig.1) (Tripathi et al., 2014; Pradeeba and sampath,2018; 2019; 2020; sampath et al., 2021) .

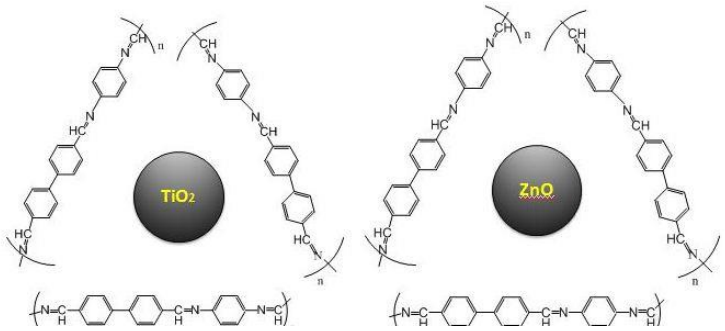

Figure 1. Structure of PNT and PNZ

2.6 .Photocatalytic Experiment

In the presence of a visible light source, batch mode photocatalytic investigations were carried out for the effective degradation of MB, BB, MG, MO, and ARS synthetic dyes utilising synthesised photocatalysts (PAZ, PNT, PNZ, TiO_2, and ZnO). Prior to irradiation, the suspension (50 mL dye solution + 20 mg photocatalyst) is stirred for 30 minutes with a magnetic stirrer (300 rpm) until adsorption-desorption equilibrium is achieved (Wahyuni et al., 2016; Azizi et al.,2021). After reaching adsorption-desorption equilibrium, the suspension was held in visible light irradiation to ensure effective photodegradation. The absorbance of the dye solution, which was pipetted out once at repeated intervals, was measured using a UV-Visible spectrophotometer.The photo deprivation efficacy R (%) was calculated using the equation (1):

$$R(\%)=\frac{C_0 - C_t}{C_0} \qquad (1)$$

C_0 symbolizes the dye concentration before irradiation and C_t indicates the dye concentration after a set period of time.

2.7.Effect of Photocatalyst dosage

100 mL of 10 mg/L MB, MG, BB, MO and ARS dyes with catalysts dosage of 0.1 g, 0.2 g, 0.3 g, 0.4 g and 0.5 g were utilised to analysis optimized pH conditions for the time period of 1-5 h.

3. Results and Discussion

3.1. Characterization of Photocatalyst

The ^{1}H-NMR spectra of monomer 4, 4'-diformyl biphenyl is shown in Fig. 2. The aromatic protons appeared a multiplet in the range δ=7.8 -7.4 ppm. A small peak at δ=10.1 ppm corresponds to the aldehyde proton attached adjacent to the aromatic ring. A strong singlet at δ=2.6 ppm represents the aromatic and the methylene protons. Thus the proposed structure of the monomer is confirmed by the ^{1}H-NMR studies.

Figure-2 ^{1}H-NMR of 4, 4'-diformyl biphenyl Monomer

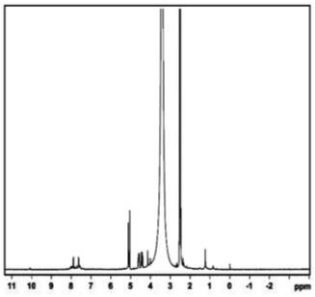

Figure-3-^{1}H-NMR of polyazomethine polymer

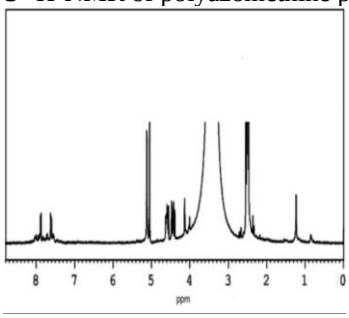

The ^{1}H-NMR of the polyazomethine polymer is shown in Fig. 3. The aromatic protons of the polyazomethine polymer showed a broad and ill-resolvedsignals at δ=7.8 -7.4 ppm. The formation of polymer is generally confirmed by the presence of broad and ill-resolved signals which is due to the entanglement of chains present in the polymer. The aldehyde proton adjacent to the aromatic ring gets disappeared with the formation of proton present in the azomethine (-N=CH-) appeared at δ= 8.1 ppm and δ= 3.10 ppm appeared for the methylene protons (Wahyuni *et a*l., 2012). Form the -N=CH-, aromatic and $–CH_2$- signals confirmed the formation of azomethine polymer. The structural characterisation of synthesised photocatalysts was reported in previous articles (Pradeeba and sampath,2018; 2019; 2020; sampath *et al*., 2021) .

3.2. Photocatalytic Activity

3.2.1. Effect of photocatalyst dosage amount

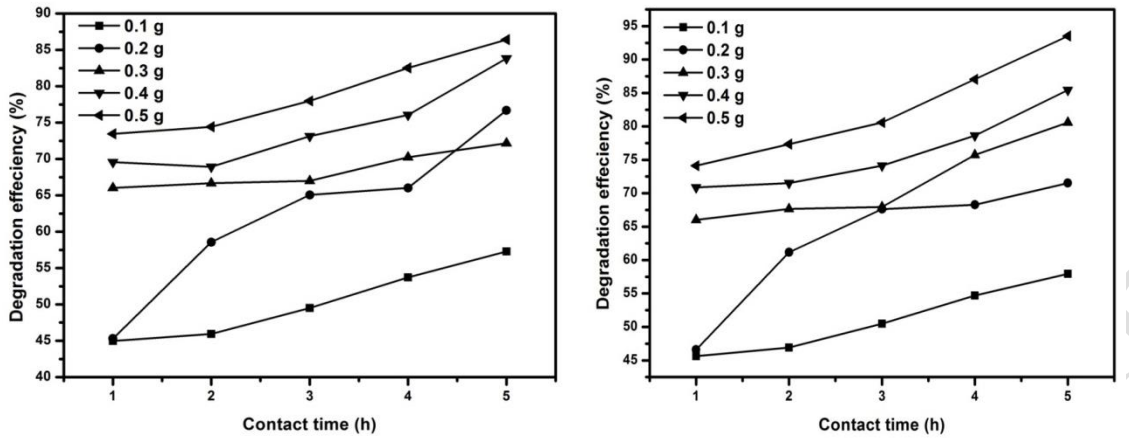

Figure 4&5. Effect of photocatalyst amount onto photodegradation of synthetic dyes using PAZ (left) and TiO_2 (right) nanoparticle .

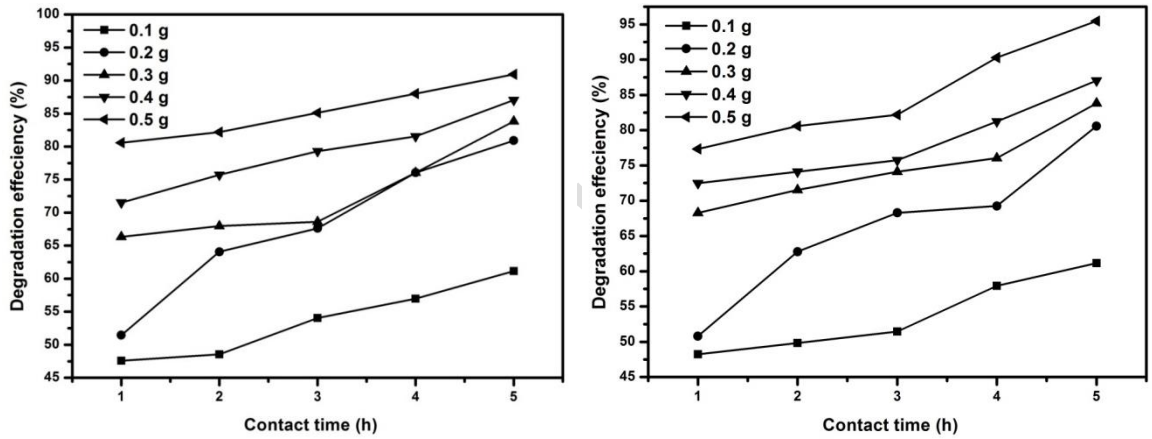

Figure 6 & 7. Effect of photocatalyst amount onto photodegradation of synthetic dyes using ZnO (left) and PNT (right) nanocomposite.

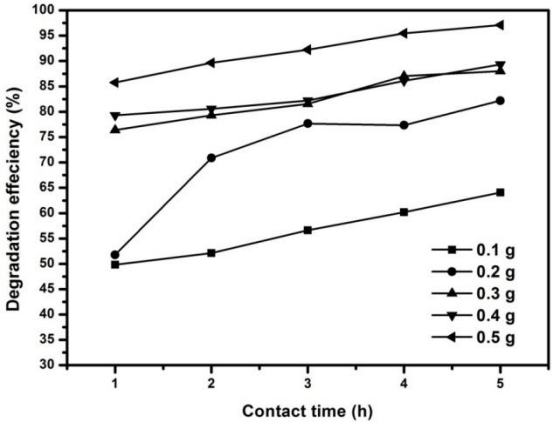

Figure 8. Effect of photocatalyst amount onto photodegradation of synthetic dyes using PNZ nanocomposite.

The effect of photocatalyst onto photodegradation of organic dyes (MB, MG, BB, MO and ARS) using PAZ, TiO_2, ZnO, PNT and PNZ synthesized materials were shown in Figures 4-8. It was obvious from the results that photodegradation increased with an increase in the catalyst dose. This is owing to the faster flow of electrons from the conduction to the valence bands, which results in faster photodegradation. However, when the amount of catalyst dose increases, the solution becomes turbid, preventing light from penetrating into the dye solution, resulting in poor degradation (Gopalappa *et al.,* 2012; Govindhan and Pragathiswaran 2016; Kim *et al*.,2016). When the photocatalyst were compared, PNT and PNZ exhibit higher degradation efficiency compared to the other synthesized materials. This is due to the presence of active sites present in the photocatalyst which is essential for the degradation of dye molecules. With increase in the amount of photocatalyst, degradation rapidly increases and reaches a plateau. This is due to the absence of no more dye molecules present in the solid-liquid interface system (Yong *et al*., 2015).

3.2. Morphological Studies

Scanning electron microscope studies was done to understand the surface morphology and characterization of catalysts, before and after chemical modification and after adsorption of dye.

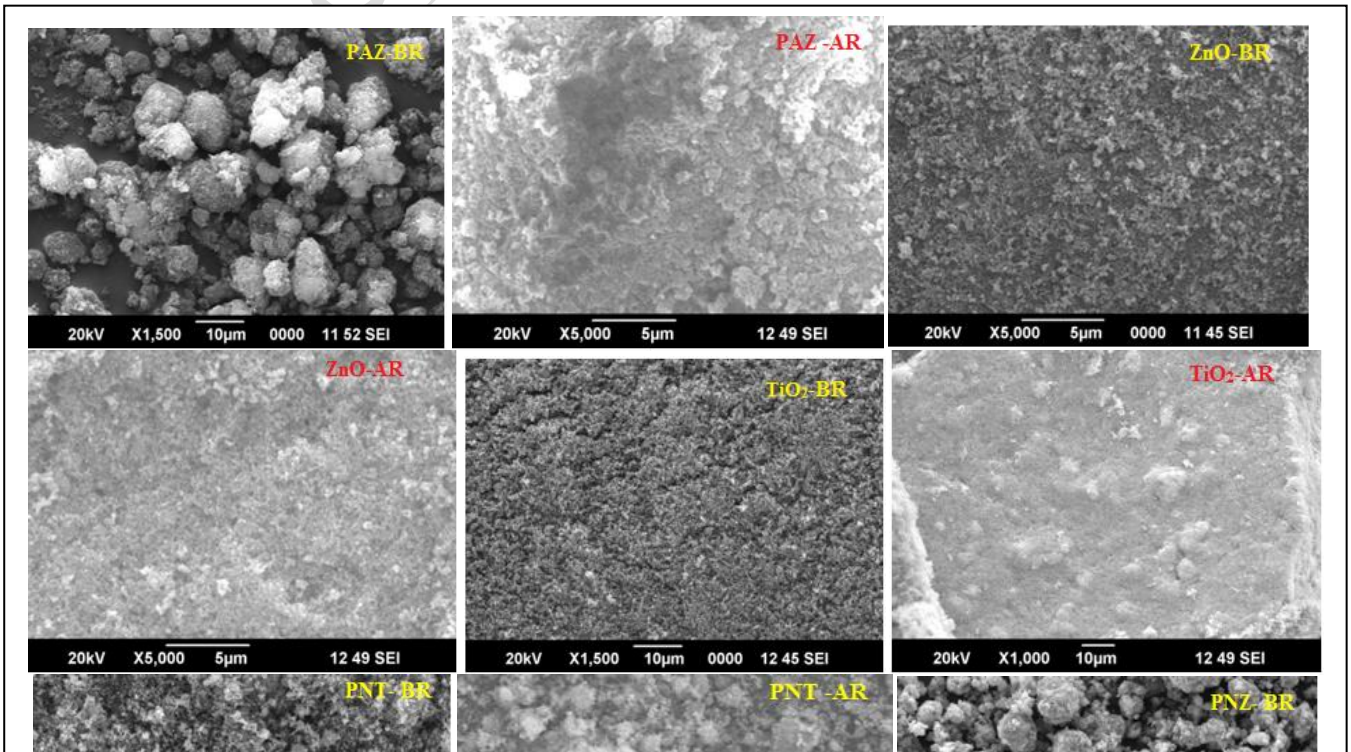

Figure 9. Scanning Electron Microscope image of PNT & PNZ nanocomposite before (BR) and after (AR) elimination of dyes

Fig.9 depicts the SEM analysis of synthesized photocatalysts (PAZ, TiO_2, ZnO, PNT and PNZ) before and after the adsorption of organic dyes. Rough permeable structure with higher craters can be perceived in SEM analysis of photocatalysts before adsorption of dye (Pathania *et al.*, 2016). It also illustrates the presence of increased surface area with irregular and interconnected pores for the efficient adsorption of dye molecules. Fig. 9 displays the formation of the agglomerate after the adsorption of dyes. Thus, the disappeared pores with a smooth surface and agglomerates confirm the dyes adsorption onto photocatalysts (PAZ, TiO_2, ZnO, PNT and PNZ).

3.3. Mechanism of Photocatalysts

The photocatalytic oxidation mechanism (Fig. 10) using semiconducting materials can be summarized as follows;

(i)Photoexcitation:When a photoelectron is promoted from the filled valence band of a semiconductor photocatalyst, such as TiO_2, to the empty conduction band as a result of irradiation, a photocatalytic reaction is activated. The energy (hv) of the absorbed photon is equal to or greater

than the band gap of the semiconductor photocatalyst (Jenwhang *et al.*, 2012). The valence band (h_{VB+}) is left with a hole due to the excitation process. As a result, an electron and hole pair (e/h_{+}) is created, as shown in the equation below.

(ii)Ionization of water:The photogenerated holes at the valence band then react with water to produce $OH^{\cdot}$ radical.

The $HO^{\cdot}$ radical formed on the irradiated semiconductor surface are verydominant oxidizing agent. It attacks adsorbed organic molecules or those that are very close to the catalyst surface non-selectively, producing them to mineralize to alevel based on their structure and steadiness level. It does not only easily attack organic contaminants but can also attack microorganisms for their higher decontamination.

(iii) Oxygenionosorption : While the photogenerated hole (h_{VB}^{+}) reacts with surface bound water or OH^{-} to produce the hydroxyl radical, electron in the conduction (e_{CB}^{-}) is taken up by the oxygen in order to generate anionic superoxide radical (O_2^{-}).

This superoxide ion may not only take part in the further oxidation process but also avoids the electron-hole recombination, thus maintaining electron neutrality within the TiO_2 molecule (Jumat *et al.*,2017).

(iv)Protonation of superoxide: The superoxide ($O_2^{-\cdot}$) produced gets protonated forming hydroperoxyl radical ($HO_2^{\cdot}$) and then consequently H_2O_2 which further separates into highly reactive hydroxyl radicals ($OH^{\cdot}$).

Both oxidation and reduction processes commonly take place on the surface of the photoexcited semiconductor photocatalyst.

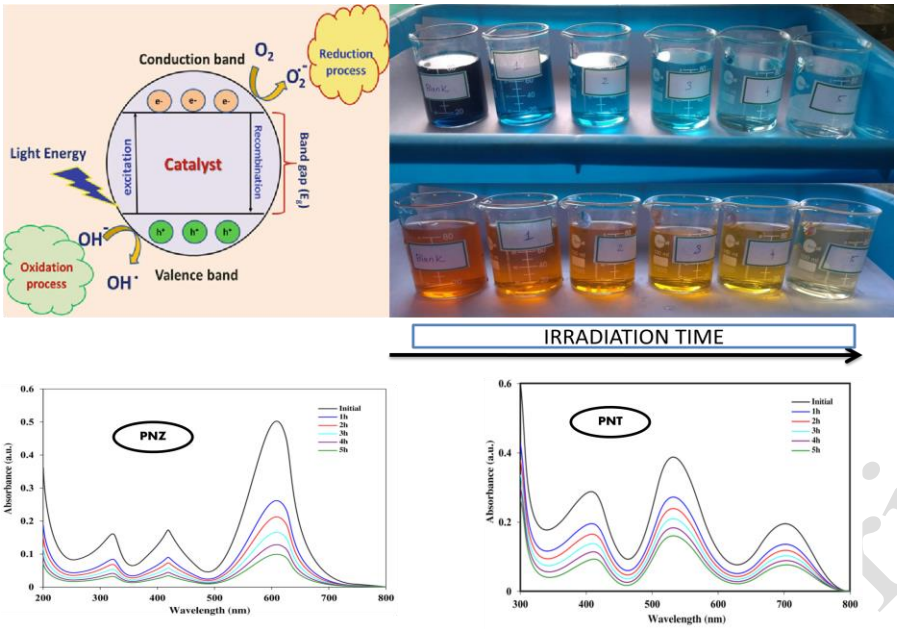

Figure 10. General mechanism of photodegradation of a dye using a photocatalyst

Therefore a semiconductor photocatalyst can take part in a redox reaction upon photo-excitation on its surface effectively. The general scheme of a photocatalytic reaction involving a semiconductor material used for the dye degradation is as follows (Eqn. 2 to 8):

$$\text{Dye} + h\upsilon \rightarrow \text{Dye}^* \quad (2)$$

$$\text{Dye}^* + TiO_2 \rightarrow \text{Dye}^{\bullet+} + TiO_2 \quad (3)$$

$$TiO_{2(e)} + O_2 \rightarrow TiO_2 + O_{2-} \quad (4)$$

$$O_{2-} + TiO_{2(e)} + 2H^+ \rightarrow H_2O_2 \quad (5)$$

$$H_2O_2 + TiO_{2(e)} \rightarrow OH + OH^- \quad (6)$$

$$\text{Dye}^{\bullet+} + O_2\ (O_{2-} \text{or } OH^-) \rightarrow \text{Organic intermediates} \quad (7)$$

$$\text{Organic intermediates} \rightarrow \text{Degraded or mineralized products} \quad (8)$$

3.4. Photocatalyst stability and reusability:

To evaluate the reusable nature of PNT and PNZ nanocomposites, 5 consecutive photocatalytic experimental runs were performed, adding recycle PNT and PNZ nanoparticles for degradation of dyes. The experiments were carried out for a total of five cycles at a dye

concentration of 50 ppm and a photocatalyst dosage of 100 mg. The photocatalyst is periodically rinsed with double distilled water and dried after each experiment. The photocatalyst is then retrieved and employed in the following experiment. After 5 cycles, there is no discernible loss of photocatalytic activity, and the moderate decline in activity is attributable to photocatalyst loss during washing (Kamil *et al.,* 2014). Thus, the photocatalyst is stable and reusable for the degradation of dyes in water.

3.5. Comparison of cationic and anionic dyes

Table 1. Maximum degradation efficiency of organic dyes using synthesized photocatalysts

Dyes	Optimized parameter	Synthesized Photocatalyst				
		PAZ	TiO_2	ZnO	PNT	PNZ
Methylene Blue (MB)	500 mg	86.40	90.93	93.52	95.46	97.08
	10 mg/L	83.81	86	85.43	87.05	90.61
	pH 11	74.57	77.96	76.27	83.05	86.44
Bismarck brown (BB)	500mg	75.55	76.66	84.44	85	96.66
	10 mg/L	72.22	75.55	77.77	84.44	89.44
	pH 11	72.22	73	77.77	83.33	85
Malachite green (MG)	500 mg	76.27	79.66	84.74	93.22	95.93
	10 mg/L	76.28	78	79	77	85
	pH 11	75.72	78.96	83.81	77.34	87.05
Methyl orange (MO)	500 mg	83.40	87	90	92.46	94.08
	10 mg/L	80.81	82.43	84.05	84.05	83.21
	pH 3	73.72	75.34	76.96	81.81	85.05
Alizarin Red S (ARS)	500 mg	73.27	81.74	76.66	90.22	92.93
	10 mg/L	80.81	82.43	84.05	84.65	82.31
	pH 3	74.57	76.27	77.96	83.05	83.44

From the above table (1) it is observed that, the maximum degradation efficiency of the photocatalysts is in the order as follows, PNZ ≥ PNT > ZnO > TiO_2> PAZ. Synthetic cationic and anionic dyes, on the other hand, were compared and examined to determine which dye degraded the most under the impact of created photocatalysts, and it was discovered that cationic dyes degraded more than anionic dyes. MB> MG> BB >MO>ARS is the order of dye removal, as seen in Fig.7.

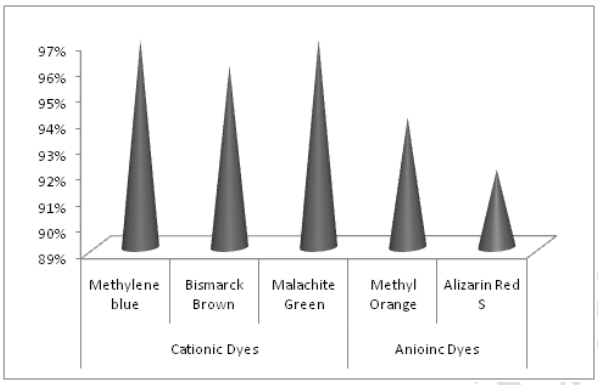

Figure 7. Efficacy of synthesized catalyst for the photodegradation of organic dyes.

4. Conclusion

The synthesized PAZ, TiO_2, ZnO, PNT and PNZ photocatalyst can be used and tested its performance with various toxic organic pollutants with well build different reactors both in large scale and small scale. The efficiency of the PAZ, TiO_2, ZnO, PNT and PNZ can be analysed and calculated with mixture of textile dyes in the presence of competing ions present in the textile effluent. As the synergic effect can play a significant role in the photodegradation process.

From the obtained observations, interferences and suggestions shows that the PAZ, TiO_2, ZnO, PNT and PNZ photocatalyst is a cost-effective alternative material which can be used as a photocatalyst for the degradation of organic dyes with the cheap and readily available source sunlight solar spectrum.

This can be a step or an economical social measure to get into a generation which effectively uses the available resources for the essential human needs rather than creating a system which can destruct the environment sooner or later causing chaos to the future generation.

Acknowledgement

The authors express their gratitude to the Hindusthan College of Engineering and Technology management and principal for their assistance in completing the project successfully.

References

Al-Kahtani, A.A. (2017), Photocatalytic Degradation of Rhodamine B Dye in Wastewater Using Gelatin/CuS/PVA Nanocomposites under Solar Light Irradiation, Journal of Biomaterials and *Nanobiotechnology*, **8**, 66-82.

Amenaghawon N.A, Osarumwense J.A., Aisien F.A. and Olaniyan, O.K. (2014), Preparation and Investigation Of The Photocatalytic Properties Of Periwinkle Shell Ash For Tartrazine Decolourisation, *Journal of Mechanical Engineering and Sciences*, **7**, 1070-1084.

Ahmad M.N., Masood ul Hassan M., Nawaz F., Anjum M.N., Iqbal S.Z., Hussain T., Mujahid A. and Farid M.F.(2022), Synthesis and characterization of poly(o-chloroaniline)/TiO_2 nanocomposites for photocatalytic degradation of direct yellow 50 dye in textile wastewater, *Global nest Journal*, **24**, 1-6.

Azizi A., Krika F. and Krika A. (2021), Efficient anionic surfactant treatment of cork for cationic dye removal from aqueous media, Global nest Journal, **23 (2),** 218-225.

Ansari M.O., Khan M.M., Ansari S.A. and Cho M.H. (2015), Polythiophene nanocomposites for photodegradation applications: Past, present and future, *Journal of Saudi Chemical Society*, **19**, 494–504.

Eskizeybek V., Sari F., Gulce H., Gulce A. and Avci A. (2012), Preparation of the new polyaniline / ZnO nanocomposite and its photocatalytic activity for degradation of methylene blue and malachite green dyes under UV and natural sun lights irradiations, *Applied catalysis B: Environmental*, **119**, 197-206.

Gopalappa H., Yogendra K., Mahadevan K.M. and Madhusudhana N. (2012), A comparative study on the solar photocatalytic degradation of brilliant red azo dye by CaO and $CaMgO_2$ nanoparticles, *International Journal of Science research*, **1**, 91-95.

Govindhan P. and Pragathiswaran C. (2016), Synthesis and characterization of TiO_2 @ SiO_2 – Ag nanocomposites towards photocatalytic degradation of rhodamine B and methylene blue, *Journal of Material science*, 60-65.

Huili C. and Chang T. (1991), Thermotropic liquid crystalline polymer. III. Synthesis and properties of poly (amide-azomethine-ester) *Journal of polymer Science*, **29**, 361-367.

Jenwhang T., Taohsieh M., and Hanchen H. (2012), Visible –light photocatalytic degradation of methylene blue with laser –induced Ag/ZnO nanoparticles, *Applied surface science*, **258**, 2796-2801.

Jumat N.A., Wai P.S., Ching J.J. and Basirun W.J. (2017), Synthesis of Polyaniline-TiO_2 Nanocomposites and Their Application in Photocatalytic Degradation, *Polymers & Polymer Composites*, **25**,507-513.

Kamil A.M., Abdalrazak F.H., Halbus A.F. and Hussein F.H. (2014), Adsorption of Bismarck Brown R Dye Onto Multiwall Carbon Nanotubes, *Environmental Analytical Chemistry*, **1**, 1-6.

Kim S.P., Choi M.Y. and Choia H.M. (2016), Photocatalytic activity of SnO_2 nanoparticles in methylene blue degradation, Materials Research Bulletin, **74**, 85–89.

Lakshmiprasanna V. and Rajagopalan V. (2016), A New Synergetic Nanocomposite for Dye Degradation in Dark and Light, *Scientific Reports,* **6**:38606, 1-10.

Liuxue Z., Peng L. and Zhixing S. (2006), Preparation of PANI- TiO_2 nanocomposites and their solid-phase photocatalytic degradation, *Polymer degradation and stability*, **91**, 2213-2219.

Muinde V.M., Onyari J.M., Wamalwa B., Wabomba J. and Thumbi R.M. (2017), Adsorption of Malachite Green from Aqueous Solutions onto Rice Husks: Kinetic and Equilibrium Studies, *Journal of Environmental Protection*, **8**, 215-230.

Mzoughi M., Anuku W., Oppong S.O.B., Shukla S.K., Agorku E.S. and Govender P.P. (2016), Neodymium doped ZrO_2-graphene oxide nanocomposies: A promising photocatalyst for photodegradation of Eosin Y Dye, *Advance Material letter*, **7**, 946-950.

Pathania D., Gupta D., Muhtase A.H., Sharma G., Kumar A., Naushad M., Ahamad T. and Alsehri S.M. (2016), Photocatalytic degradation of highly toxic dyes using chitosan-g-poly (acrylamide)/ZnS in presence of solar irradiation, *Journal of photochemistry and photobiology A: Chemistry*, **329**, 61-68.

Patil M.R. and Shrivastava V.S. (2015), Adsorptive removal of methylene blue from aqueous solution by polyaniline-nickel ferrite nanocomposite: a kinetic approach, *Desalination and Water Treatment*, 1-9.

Perju E., Ghimpu L., Hitruc G., Harabagiu V., Bruma M. and Marin L. (2015), Organic–inorganic hybrid nanomaterials based on inorganic oxides and a mesomorphic polyazomethine, *High Performance Polymers*, **27**, 546–554.

Pradeeba S.J. and Sampath K. (2018), A Comparative Study Of Photo-Catalytic Degradation Efficiency Of Methylene Blue Dye In Waste Water Using Poly(Azomethine)/ZnO Nanocomposite And Poly(Azomethine)/TiO_2 Nanocomposite, *Journal of ovonic research*, 14 **(3),** 243-259.

Pradeeba S.J. and Sampath K. (2019), Photodegradation efficiency of methyl orange and Alizarin Red S in waste water using poly(azomethine)/TiO_2 nanocomposite, *AIP Conference Proceedings*, **2162** (1), 020028.

Pradeeba S.J. and Sampath K. (2019), Synthesis and Characterization of Poly (azomethine)/ZnO Nanocomposite Toward Photocatalytic Degradation of Methylene Blue, Malachite Green, and Bismarck Brown, *Journal of Dynamic Systems, Measurement and Control*, **141(5**), 051001.

Pradeeba S.J. and Sampath K. (2020), Degradation of methyl orange and Alizarin Red S from waste water using poly (azomethine)/ZnO nanocomposite as a photocatalyst, *AIP Conference Proceedings*, **2270** (1)**,** 110001.

Pradeeba S.J., Sampath K. and Kalapriya K. (2020), Photocatalytic degradation efficiency of malachite green in aqueous medium using poly (azomethine)/ZnO nanocomposite, *AIP Conference Proceedings*, **2142** (1)**,** 150003.

Pradeeba S.J., Sampath K. and Ramadevi A. (2018), Photo-catalytic degradations of methylene blue, malachite green and Bismarck brown using poly (azomethine)/TiO_2 nanocomposite, *Cluster computing*, 3893-3909.

Riaz U., Ashraf S.M. and Kashyap J. (2015), Role of Conducting Polymers in Enhancing TiO_2-based Photocatalytic Dye Degradation: A Short Review, *Polymer-Plastics Technology and Engineering*, **54**, 1850–1870.

Sampath Krishnan., Pradeeba S.J., Karunakaran, A., Kumarasamy, K., Mei-Ching Lin. (2021), The effect of pH on the photocatalytic degradation of cationic and anionic dyes using polyazomethine/ZnO and polyazomethine/TiO_2 nanocomposites, *International Journal of Applied Science and Engineering*, **18 (5),** 1-8.

Tripathi S.M., Tiwari D. and Ray A. (2014), Electrical Conductivity of polyazomethine nanocomposite, *Indian Journal of Chemistry*, **53A**, 1505-1512.

Vasanthi B.J. and Ravikumar L. (2013), Synthesis and Characterization of Poly(azomethine ester)s with a Pendent Dimethoxy Benzylidene Group, *Open Journal of Polymer Chemistry*, **3**, 1-8.

Wahyuni S., Kunarti E.S., Swasono R.T. and Kartini I. (2018), Characterization and Photocatalytic Activity of TiO_2(rod)-SiO_2-Polyaniline Nanocomposite, Indonesian *Journal of Chemistry*, **18 (2)**, 321 – 330.

Yong L., Zhanqi G., Yuefei J., Xiaobin H., Cheng S., Shaogui Y., Lianhong W., Qingeng W. and Fang D. (2015), Photodegradation of malachite green under simulated and natural irradiation: Kinetics, products, and pathways, *Journal of Hazardous Materials*, **285**, 127–136.

Zhu J., Jiang G., Qian F., Ling C. and Ming Z. (2010), Effect of key operational factors on decolorization of methyl orange during H_2O_2 assisted CdS/TiO_2/ polymer nanocomposite thin films under simulated solar light irradiation, *Separation and purification technology*, **74**, 187-194.